SAND2017-4249C

Exceptional service in the national interest

Sandia National Laboratories

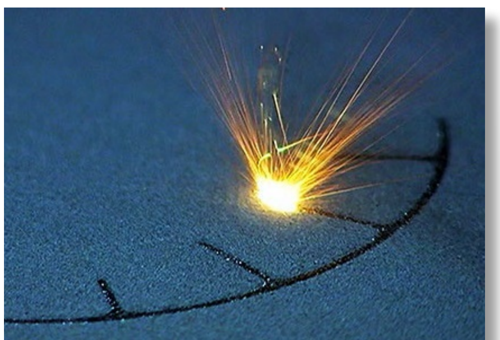

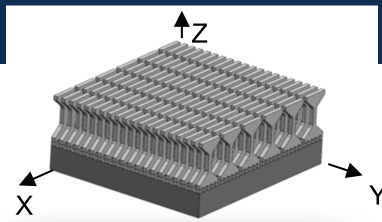

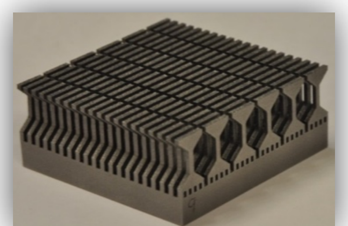

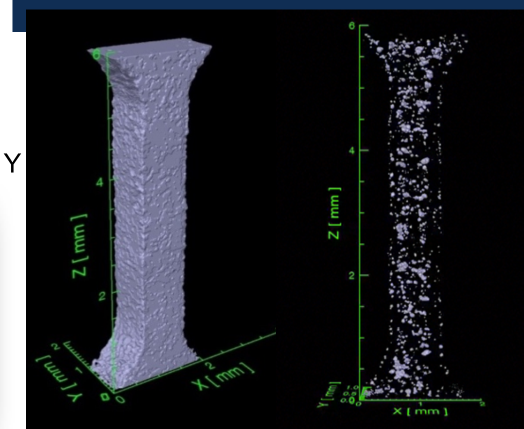

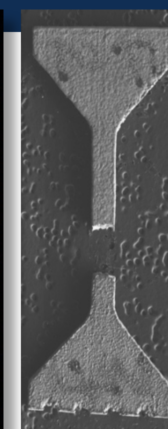

Quantifying Defect Presence in an Additively Manufactured Precipitation Hardened 17-4 Stainless Steel

Jonathan Madison[1], Laura Swiler[2], Olivia Underwood[1], Brad Boyce[1], Bradley Jared[3], Jeff Rodelas[4], Bradley Salzbrenner[1]

Sandia National Laboratories, Albuquerque, NM

U.S. DEPARTMENT OF ENERGY

NNSA National Nuclear Security Administration

Sandia National Laboratories is a multi-program laboratory managed and operated by Sandia Corporation, a wholly owned subsidiary of Lockheed Martin Corporation, for the U.S. Department of Energy's National Nuclear Security Administration under contract DE-AC04-94AL85000. SAND NO. 2017-XXXXC

Sandia National Laboratories

Acknowledgements

- Carl Jacques
- Joseph Romero
- Burke Kernan

Sandia National Laboratories

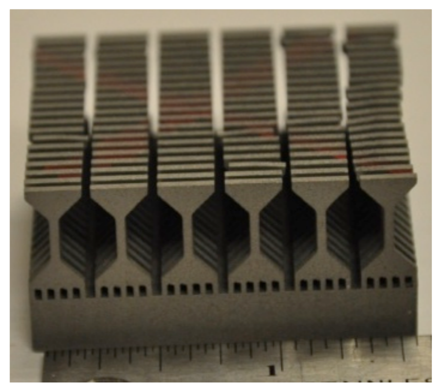

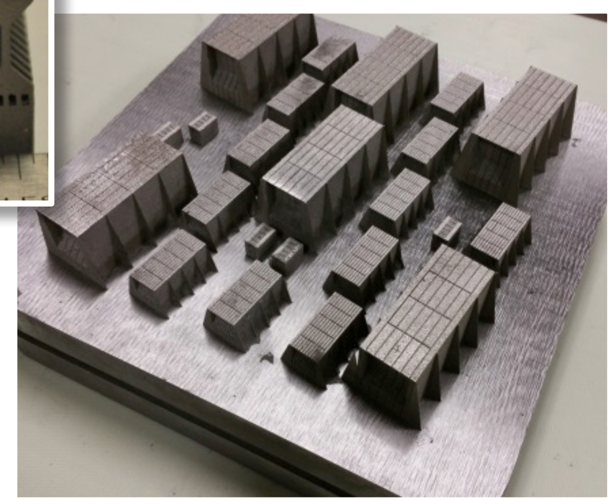

LDRD
LABORATORY DIRECTED RESEARCH & DEVELOPMENT

Outline

- Additive Manufacturing & Critical Defects
- High-Throughput Mechanical Testing
- Metallurgical Assessments
  - Microhardness
  - Microstructure
  - Composition
  - Surface Finish & Failure Modes
  - Fractography
- Micro-Computed Tomography
  - Defect Quantification
  - Correlations with Mechanical Response
- Conclusions

Identify *Critical* Defects

- Characterize, predict & control for laser PBF
- Quantify "signatures"
  - destructive
    - high throughput testing (HTT), fractography, metallography, serial sectioning
  - non-destructive
    - computed tomography (CT), density, process controlled resonance testing (PCRT)
  - what can we ID both accurately & efficiently?
- Understand mechanistic impacts on properties
  - characterize stochastics
  - build process-structure-property relationships to predict margins & reliability
  - **provide scientific basis for qualification of AM metals**

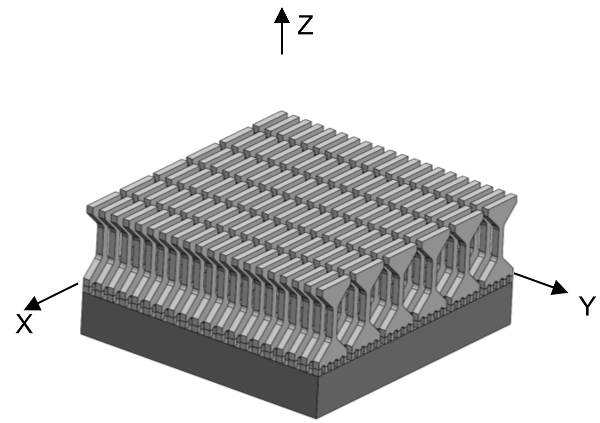

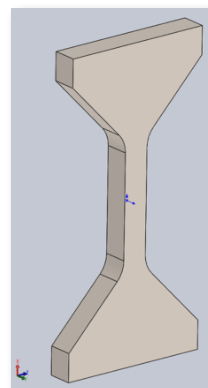

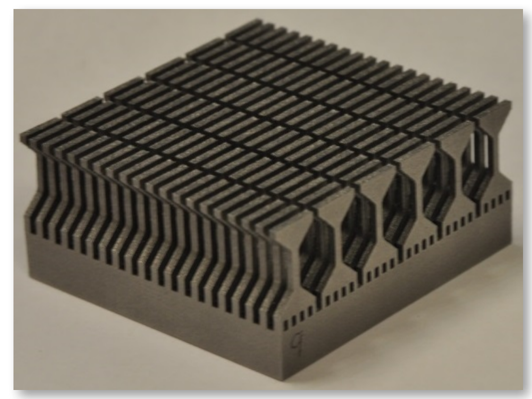

1x1 mm gage section sample

17-4 PH Stainless Steel

High-Throughput Mechanical Testing

- Quantifying mean, outliers & probabilities
  - >100 samples / test condition
  - external vendor sources
  - compared against wrought
- Defect dominated failure
  - limited area reduction
  - observed ductile dimples & shear rupture planes
  - voids & lack-of-fusion boundaries are likely crack nucleation sites

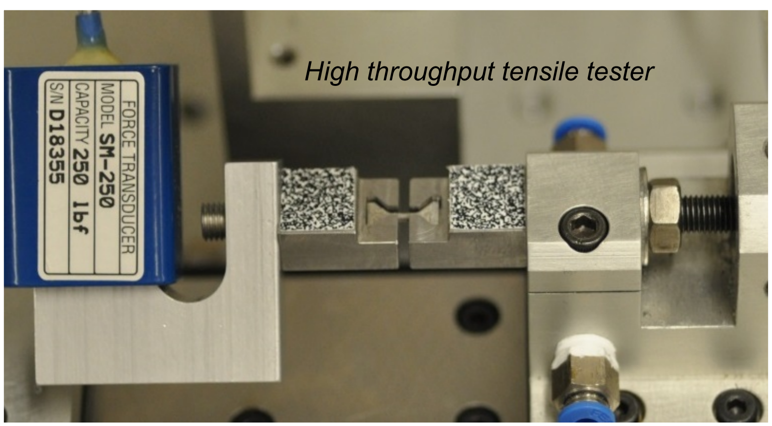

H900 data for vendor 1 (top left), vendor 2 (top right) & wrought (bottom)

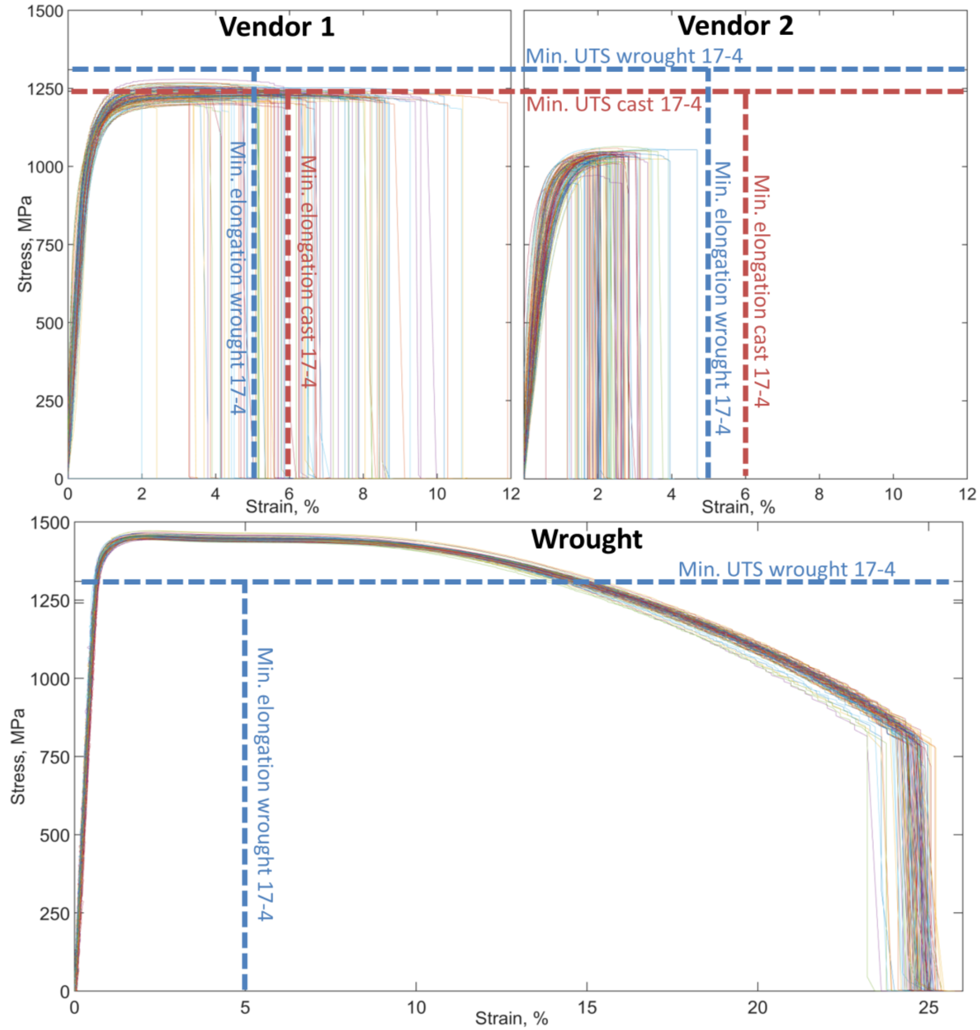

AMS spec for H900: modulus = 197 MPa, yield = 1172 MPa, UTS = 1310 MPa, strain at failure = 5%

Metallurgical Assessments

- Microhardness
- Microstructure
  - optical, SEM, EBSD, WDS micro-probe
- Composition
  - LECO combustion, ICP mass-spec, XRD
  - powder analysis

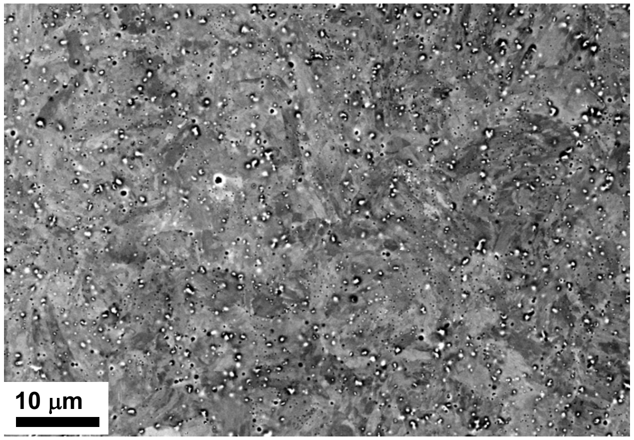

Electron backscatter channeling contrast imaging of as-printed vendor 2 17-4PH shows appreciable fraction of retained austenite

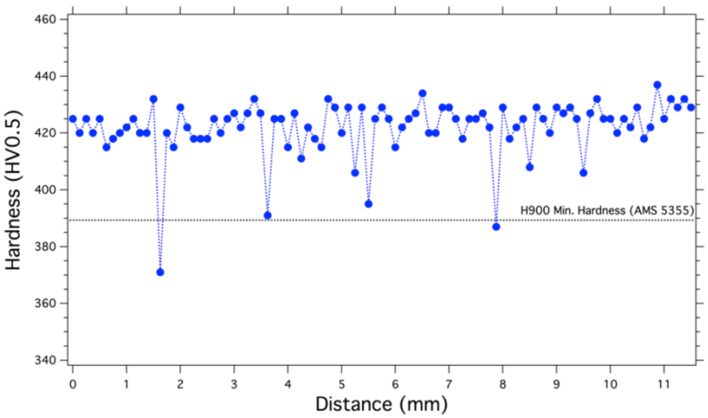

vendor 1, H900 microhardness along dogbone length

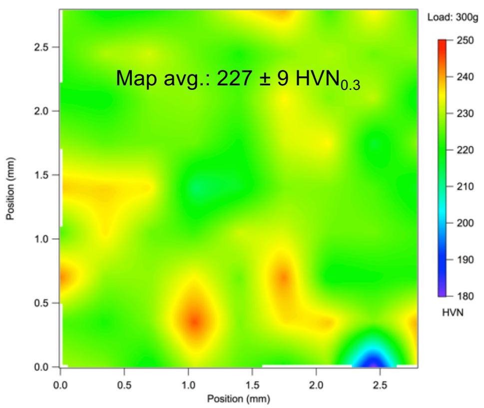

vendor 2, as-printed microhardness on gauge cross section

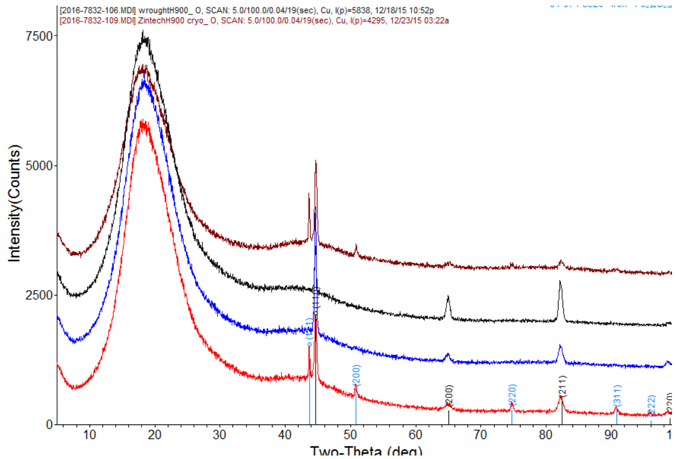

bulk XRD analysis for vendor 2

Microhardness

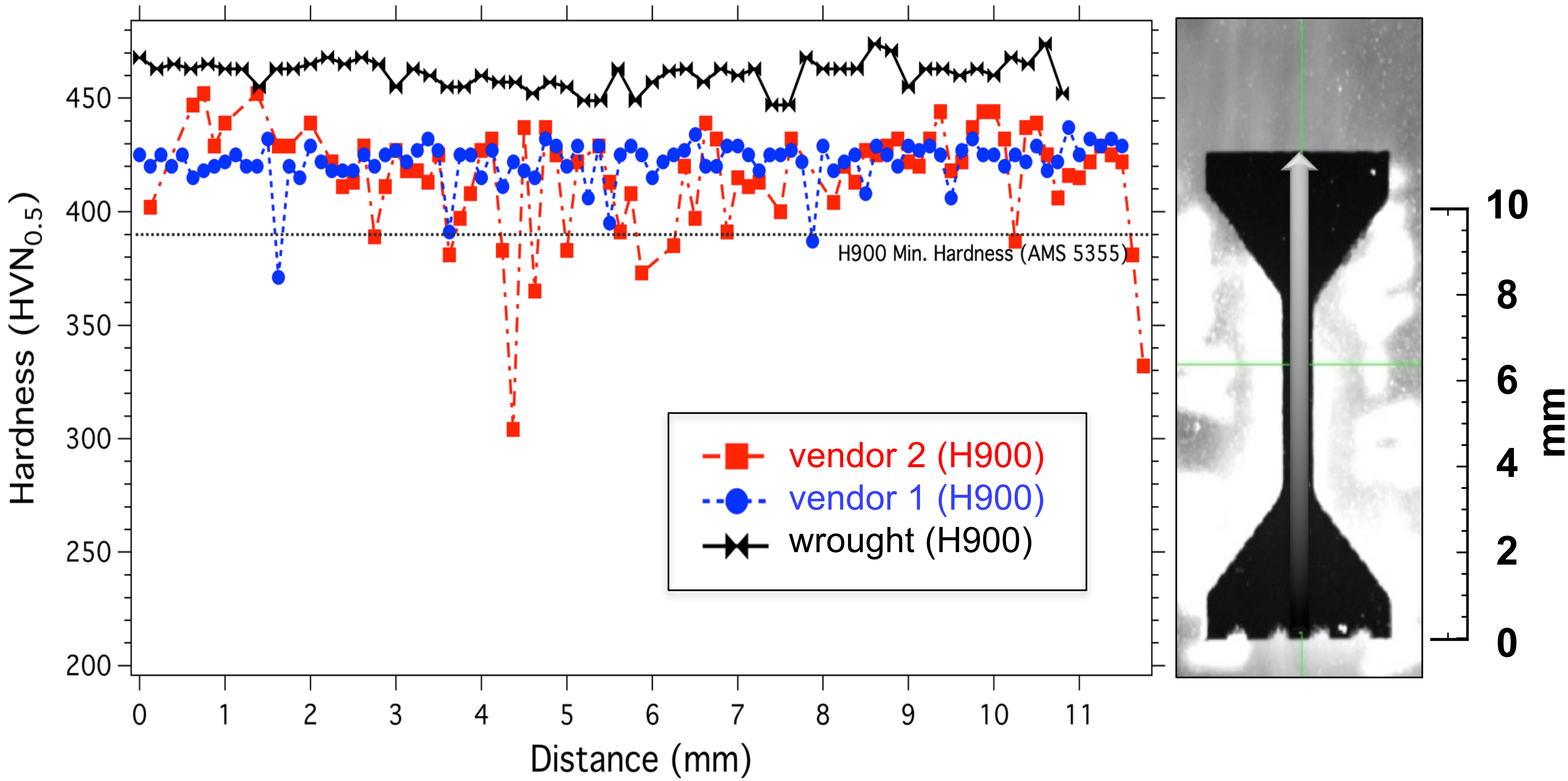

Greater variability in vendor 2 material but no intrinsic difference in hardness in comparison to vendor 1

Microstructure

Vendor 1

martensitic microstructure
submicron Nb-rich carbides

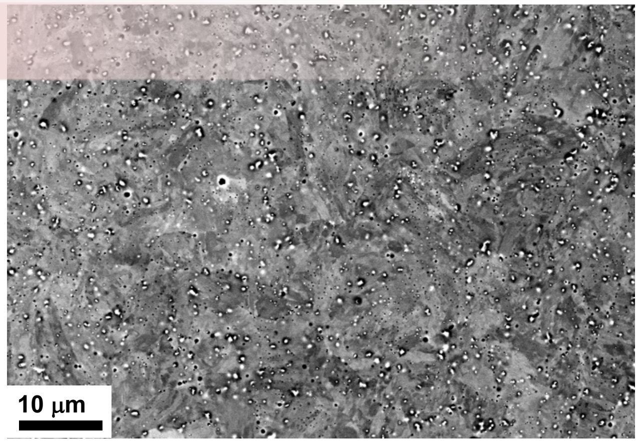

SHT + H900 age
Backscatter electron micrograph

Vendor 2

martensitic lath microstructure
submicron Nb-rich carbides

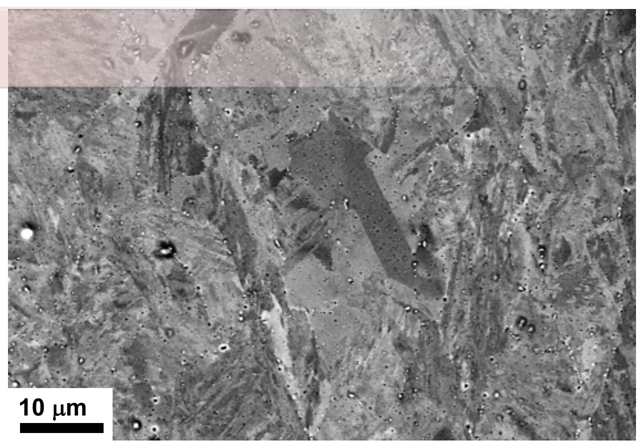

SHT + H900 age
Backscatter electron micrograph

Element	Vendor 1, run 2 (wt%)	Vendor 2, As Printed (wt%)
Cr	16.64	16.51
Mo	0.045	0.17
Si	0.38	0.62
Nb	0.3	0.29
V	0	0
W	0	0
Ti	0	0
Ta	0	0
Al	0	0
Ni	4.24	4.53
Mn	0.24	0.46
C	0.012	0.021
N	0.056	0.15
Co	0	0
Cu	4.05	4.08
P	0.019	0.023
S	0.003	0.006
O	0.100	0.083

bulk chemical analysis

Microstructure

Vendor 1

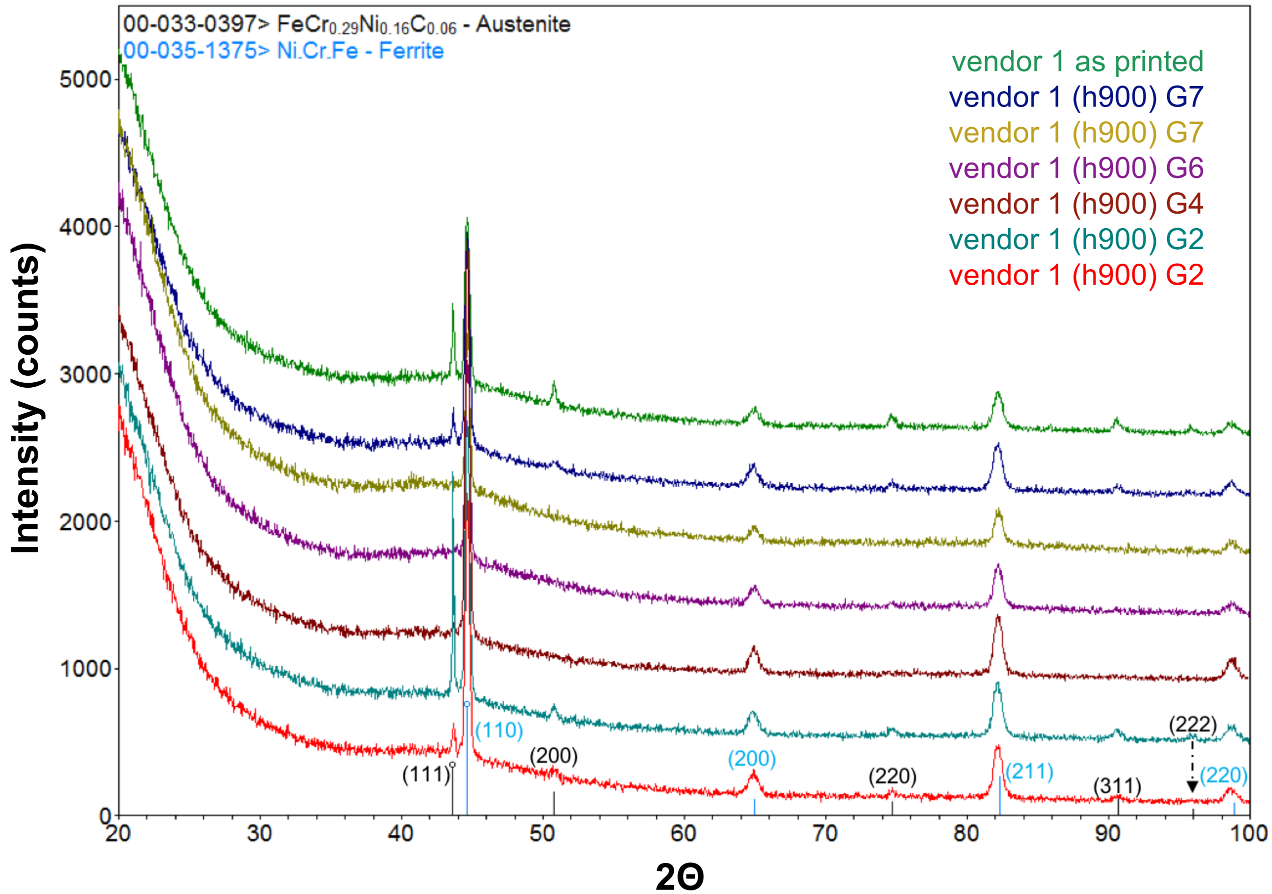

- Significant amounts of retained austenite in vendor 2 material pre- and post heat treatments

Austenite largely absent in heat treated wrought and heat treated vendor 1 material

When observed in vendor 1 material, via XRD, austenite was seen to exist in the range of 12% or less

Microstructure

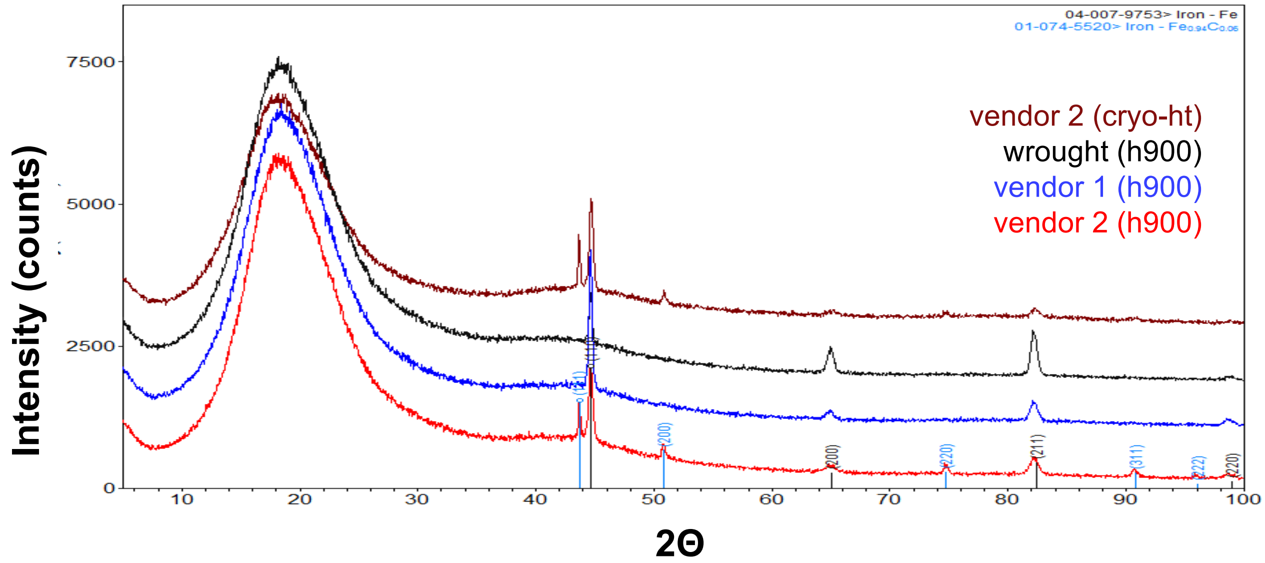

- Significant amounts of retained austenite in vendor 2 material pre- and post heat treatments
- Austenite largely absent in heat treated wrought and heat treated vendor 1 material

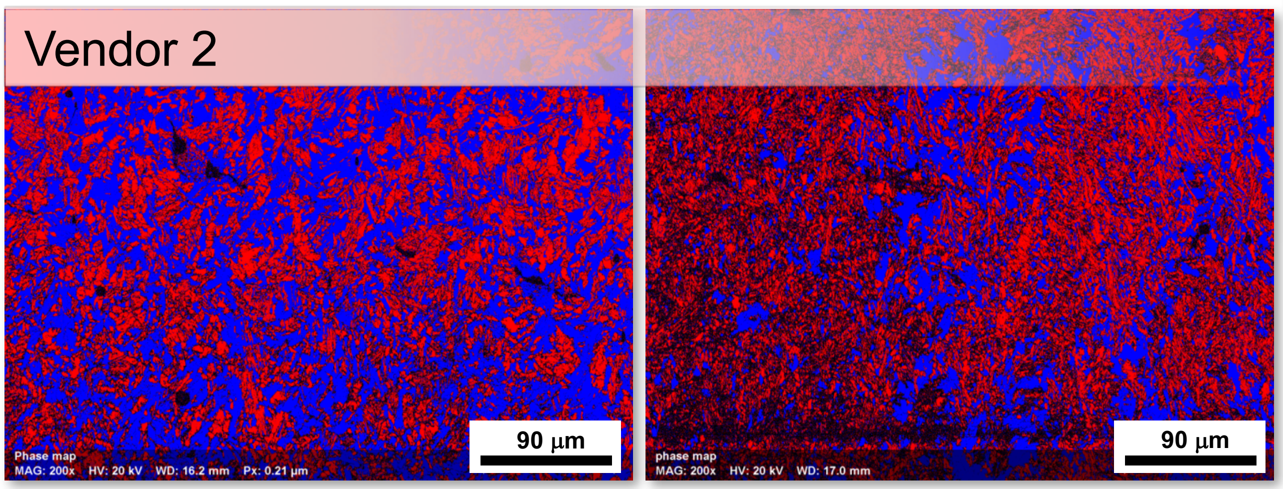

as-printed, 47% austenite

SHT + H900 age *43% austenite*

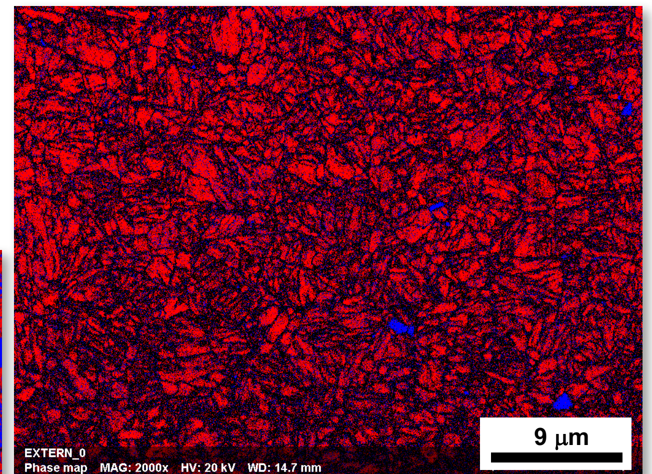

wrought sheet shows fine-grained martensite

Blue *= austenite (FCC)*
Red *= martensite / ferrite (BCC)*
Black *= non-indexed*

Composition

- Shows high austenite stability & propensity for primary austenite solidification

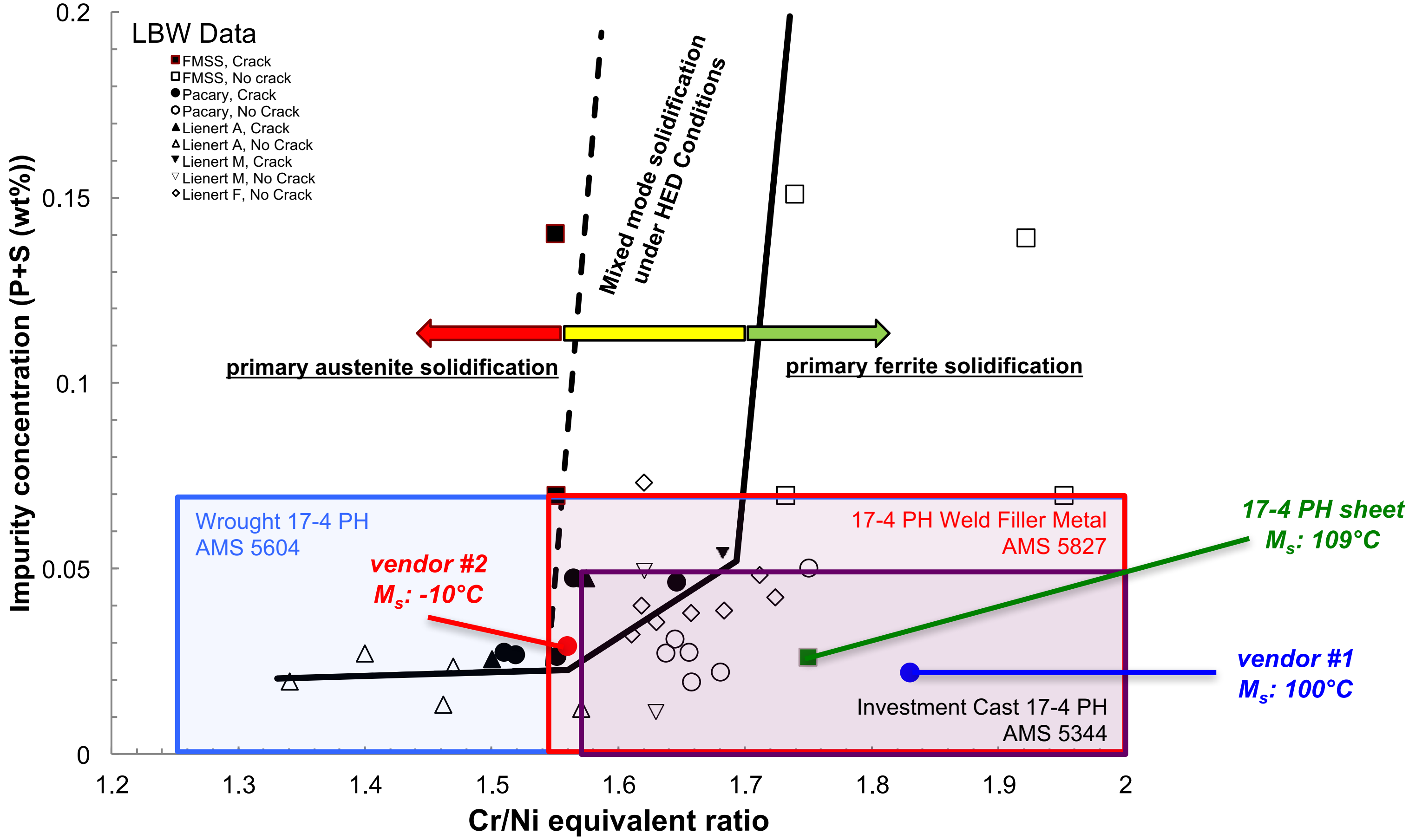

Eichelman & Hull: M_s (ºC) = 1302 – 42[Cr] – 61[Ni] – 33[Mn] – 28 [Si] – 1667[C+N]

Surface Finish & Failure Modes

Vendor 1

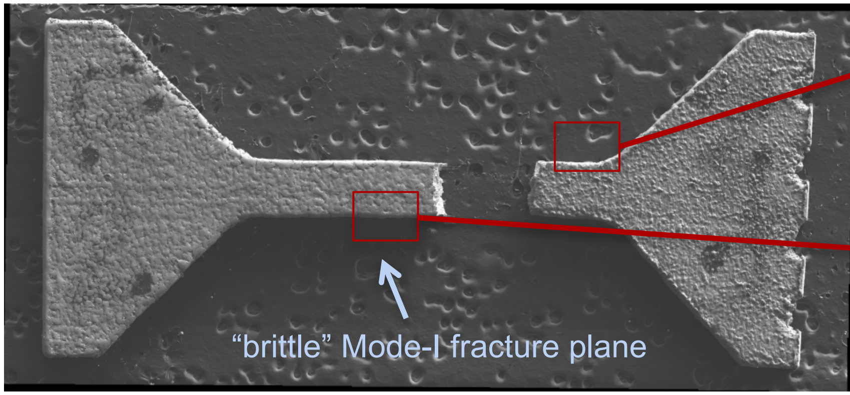

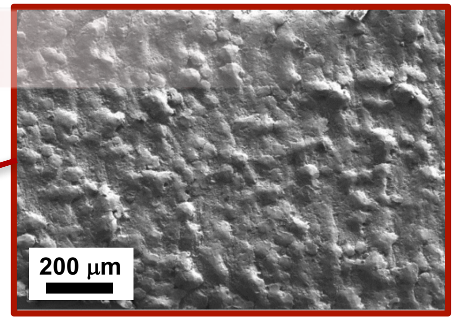

Exterior surface
(greater bead-blasting)

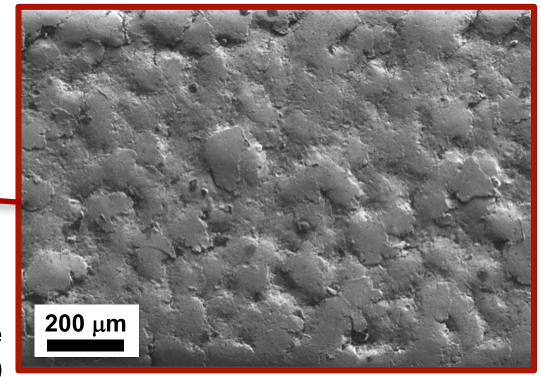

Interior surface
(lesser bead-blasting)

Surface roughness (Ra) 5.6 mm (± 0.1 mm)
Maximum peak height (Rp) of 36 mm (± 0.6 mm)

Vendor 2

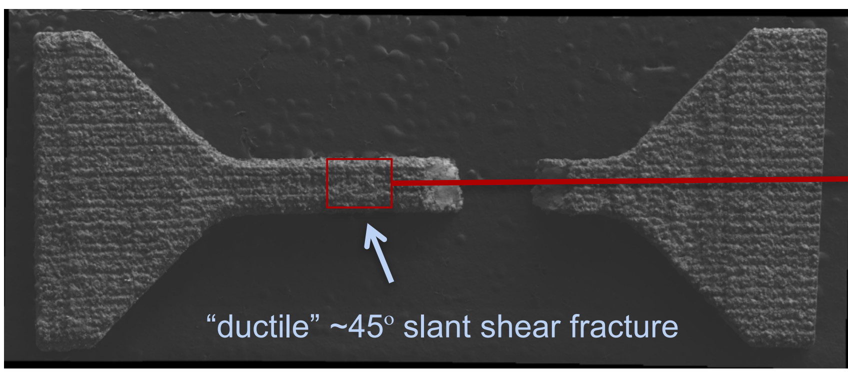

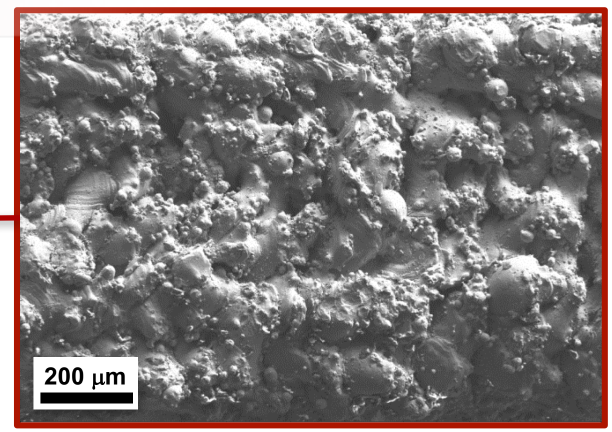

All surfaces (As printed)

Surface roughness (Ra) 18 mm (± 0.1 mm)
Maximum peak height (Rp) of 82 mm (± 0.6 mm)

Surface Finish & Failure Modes

Vendor 1

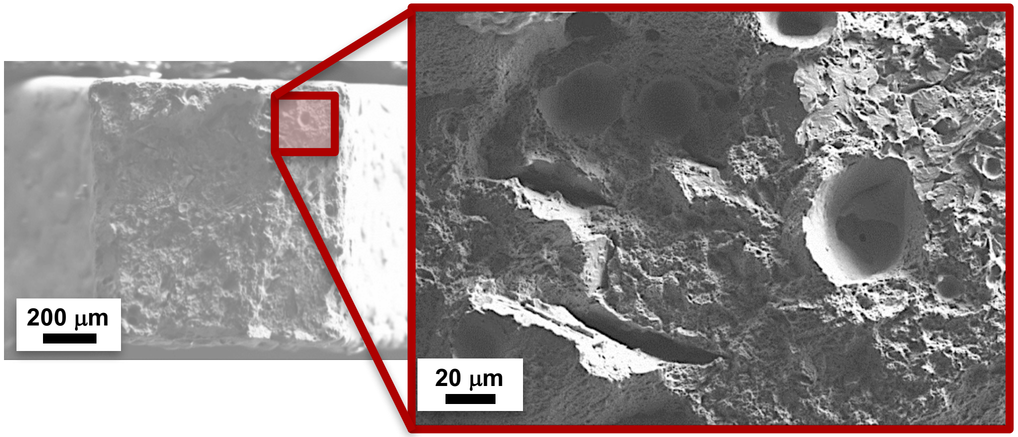

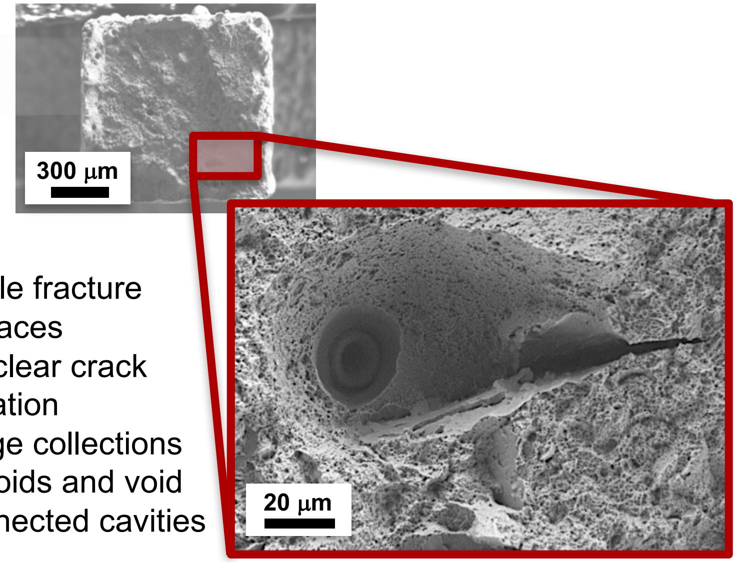

- Brittle fracture surfaces
- No clear crack initiation
- Large collections of voids and void connected cavities

Vendor 2

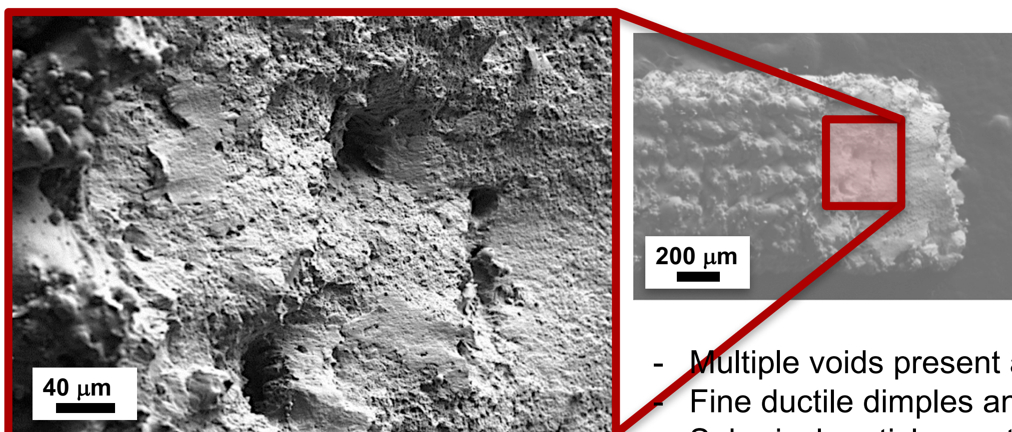

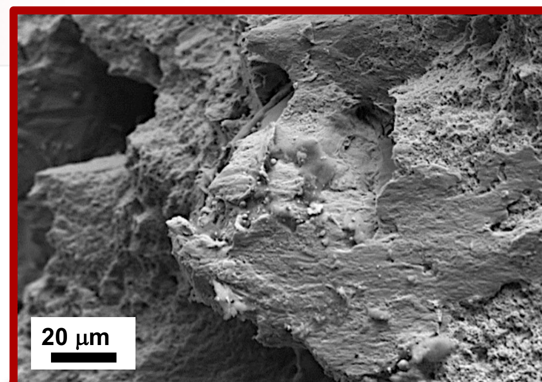

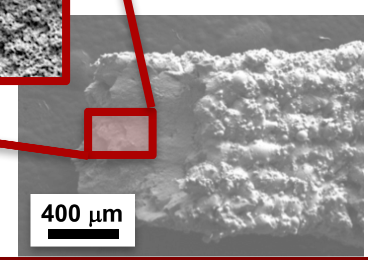

- Multiple voids present at fracture surface
- Fine ductile dimples and shear rupture planes
- Spherical particles on the fracture surface

Fractography

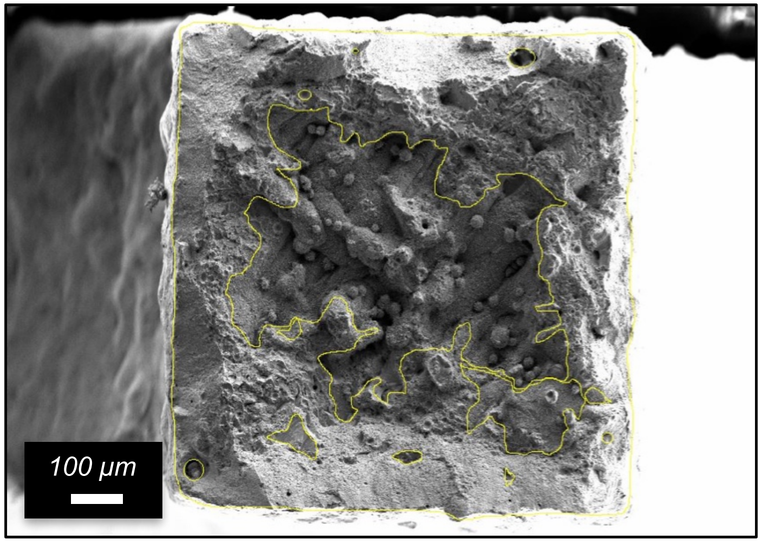

Strain-to-Failure: 10.1%

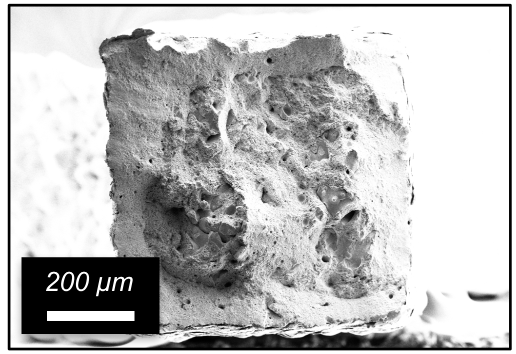

- ~6 area% of fracture surface contains lack-of-fusion defects
- Partial shear lip formation

Strain-to-Failure: 1.8%

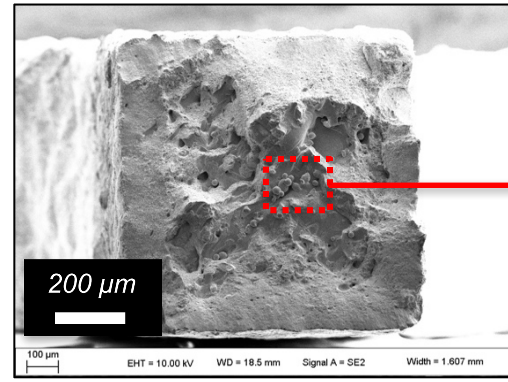

- ~22 area% of fracture surface contains lack-of-fusion defects
- Gross defects primarily all internal
- No shear lip formation—macroscopically brittle failure

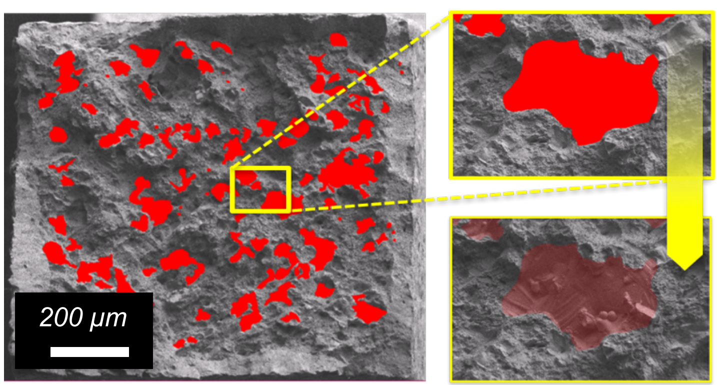

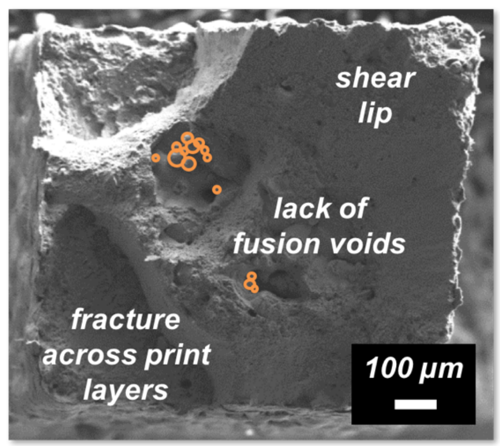

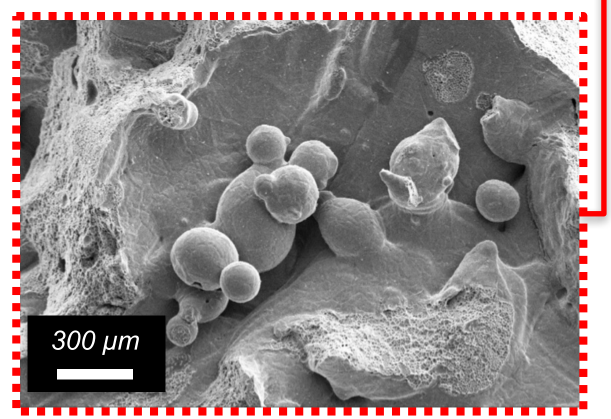

μ-Computed Tomography

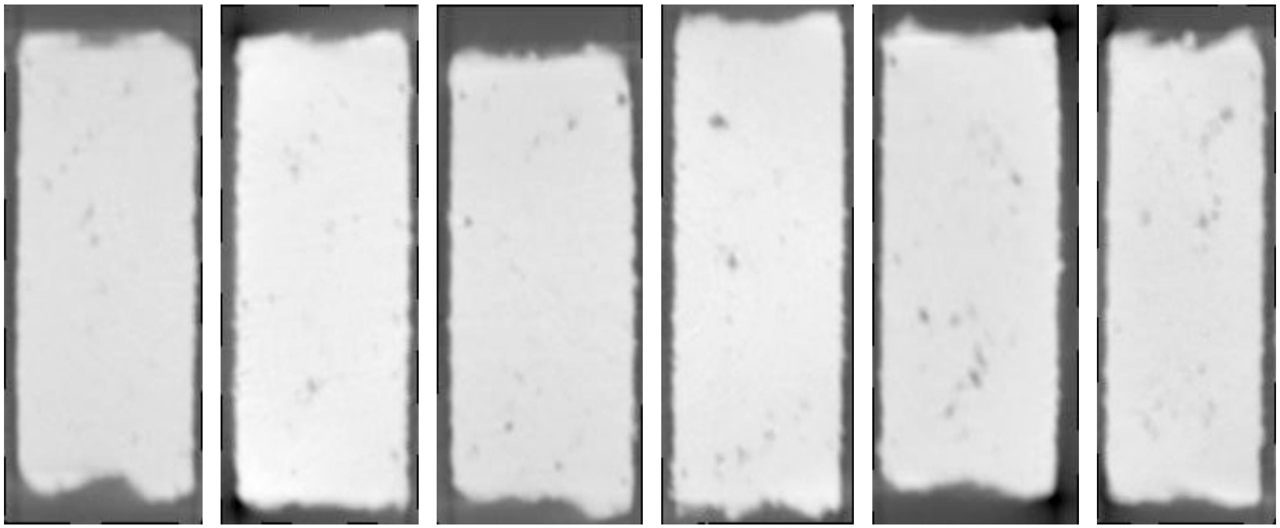

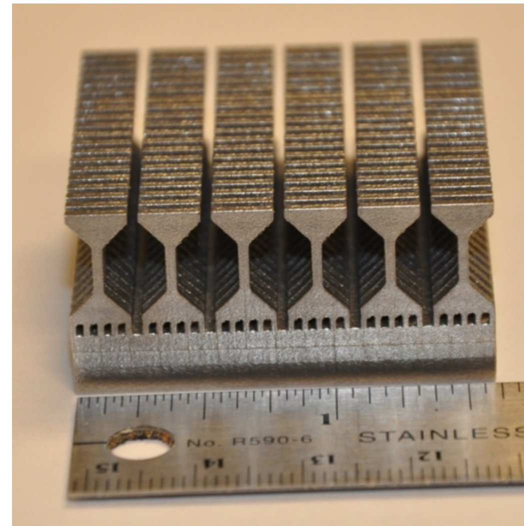

17-4 PH AM Tensile Dogbones

AM sample

6 columns x 20 rows
120 tensile dog bones per build
1 mm x 1 mm tensile gage section

μCT data

resolutions of 7-10 μm per voxel edge
defect threshold > 20μm ESD
~ 60 MB per dataset (image stack)
7+ GB for μcT data of entire build group

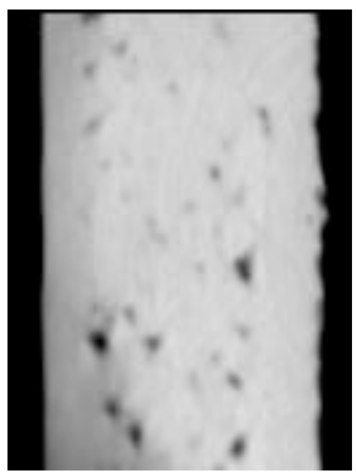

North Star Imaging, Inc. X50 XViewCT Cabinet System
YXLON Demountable Microfocus Tube (10-225kV)

3D Reconstruction of Pore Defects

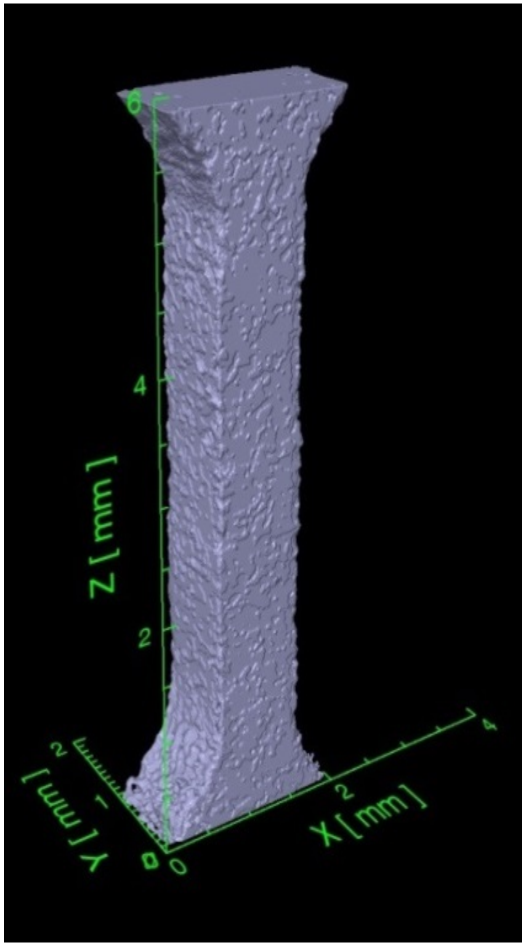

3D µCT surface render

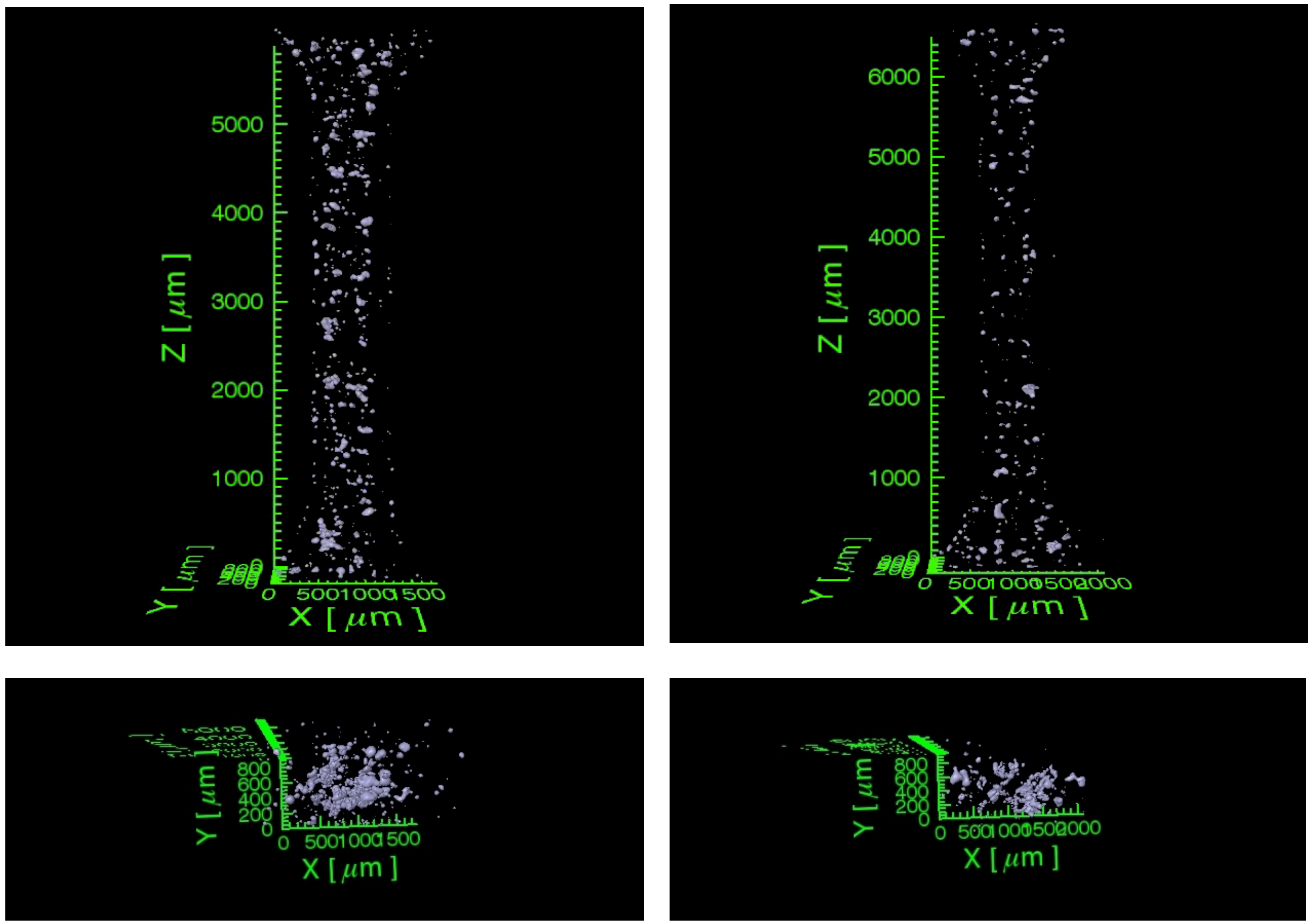

3D µCT internal porosity

Tremendous variation in pore content from sample to sample
Pore locations reminiscent of AM laser raster pattern

Defect Quantification

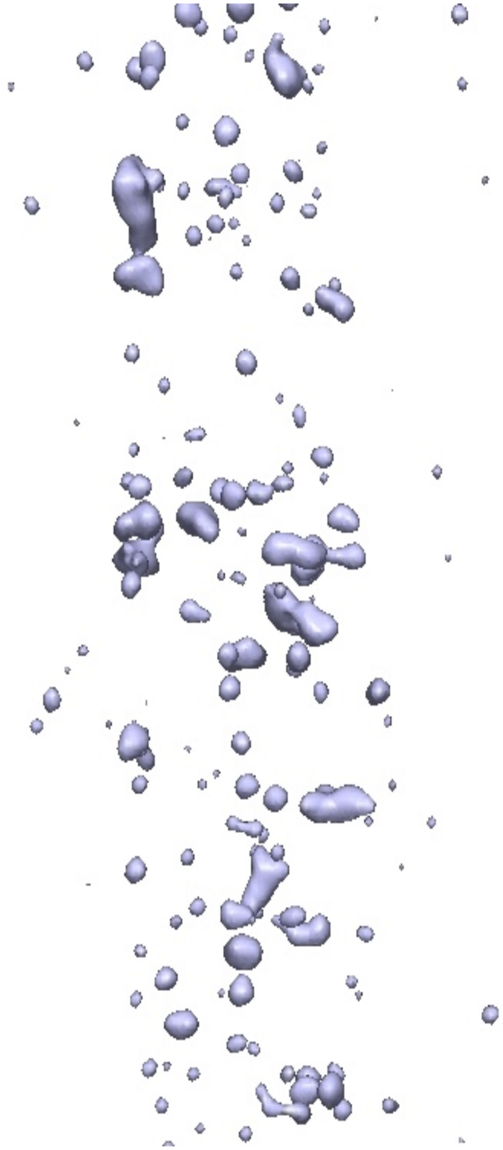

How do we *best* represent the defect populations present?

Defect Quantification

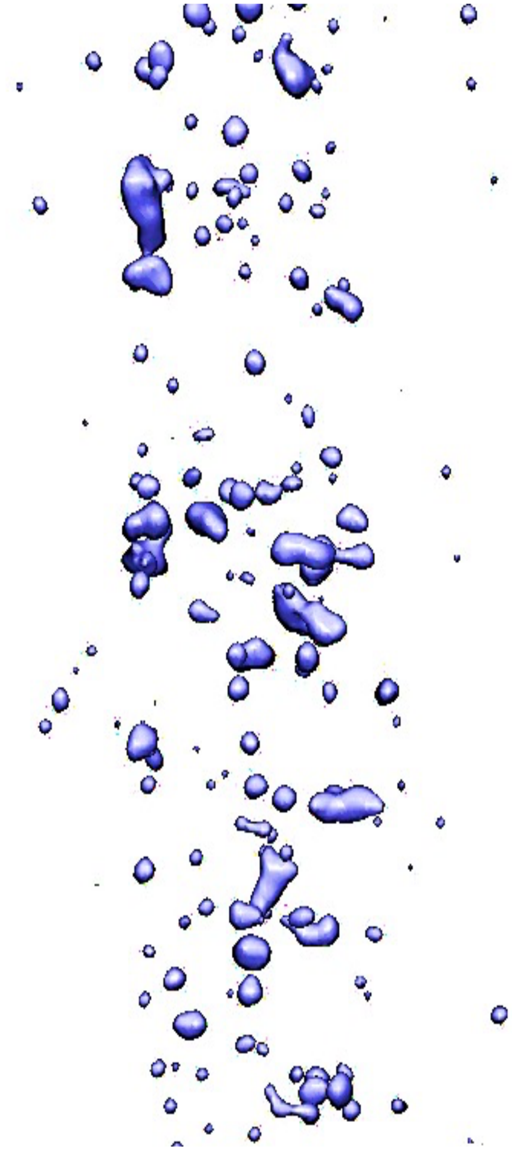

- **Total Volume of Defects *(V_{tot})***

How do we *best* represent the defect populations present?

Defect Quantification

- **Total Volume of Defects** ***(V_{tot})***
- **Pore Volume Fraction** ***(V_{fract})***

How do we *best* represent the defect populations present?

Defect Quantification

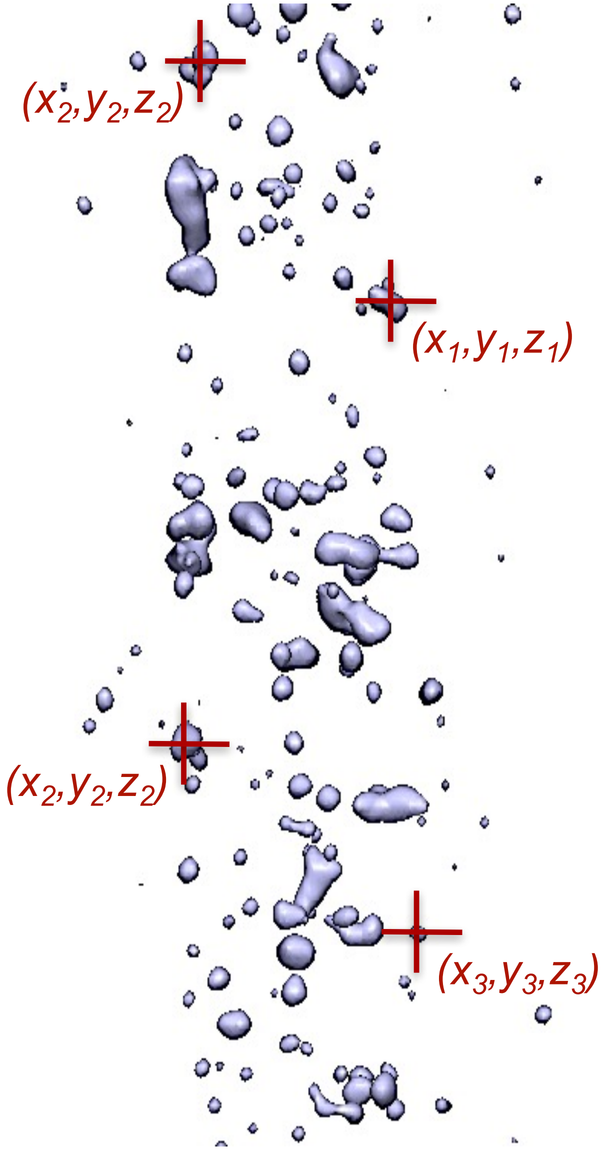

- **Total Volume of Defects *(V_{tot})***
- **Pore Volume Fraction *(V_{fract})***
- **Spatial Location of Pores *(x, y, z)***

How do we *best* represent the defect populations present?

Defect Quantification

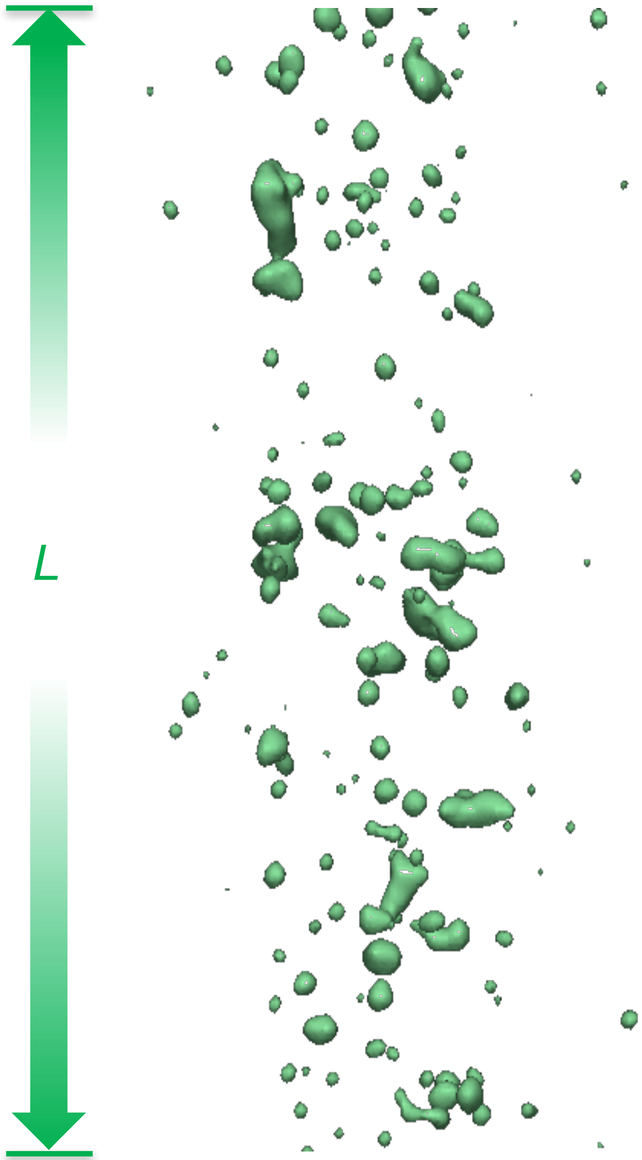

- Total Volume of Defects *(V_{tot})*
- Pore Volume Fraction *(V_{fract})*
- Spatial Location of Pores *(x, y, z)*
- Total Number of Defects *(N)*
- Total Defects/Length *(N/L)*

How do we *best* represent the defect populations present?

Defect Quantification

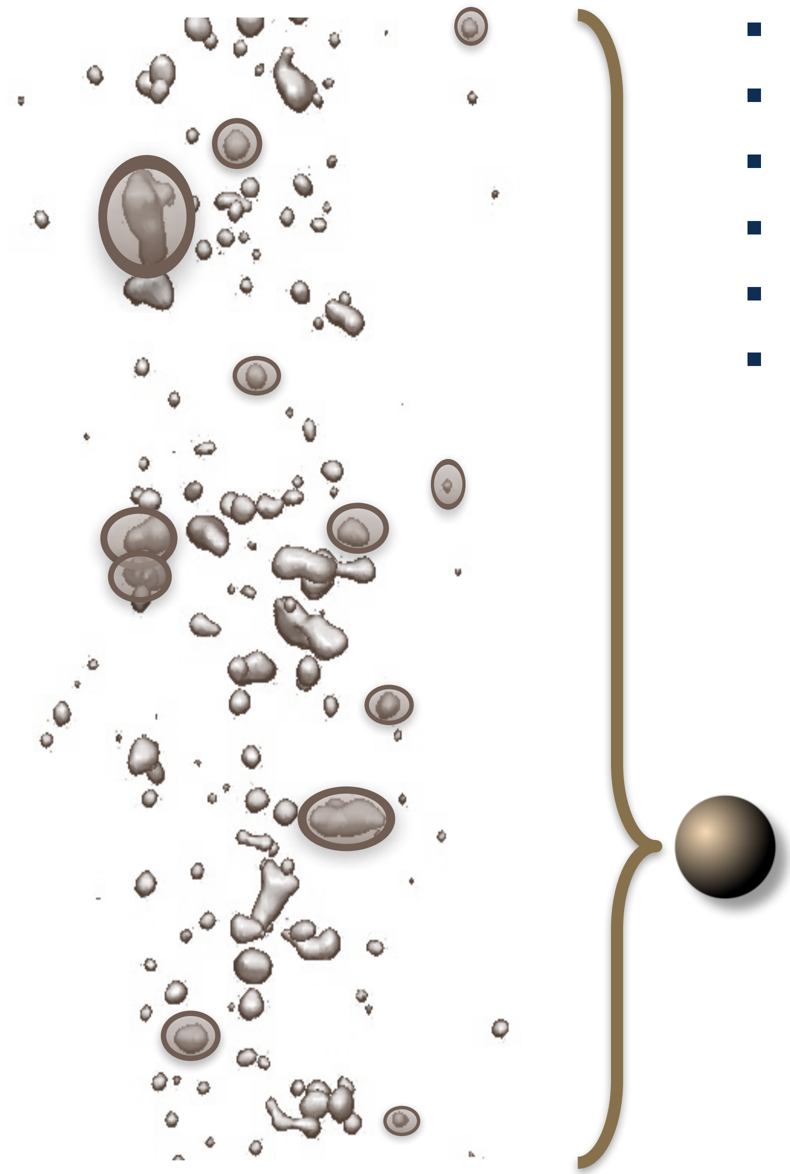

- Total Volume of Defects (V_{tot})
- Pore Volume Fraction (V_{fract})
- Spatial Location of Pores (x, y, z)
- Total Number of Defects (N)
- Total Defects/Length (N/L)
- Average Defect Volume ($V_{ave.}$)*

How do we *best* represent the defect populations present?

Defect Quantification

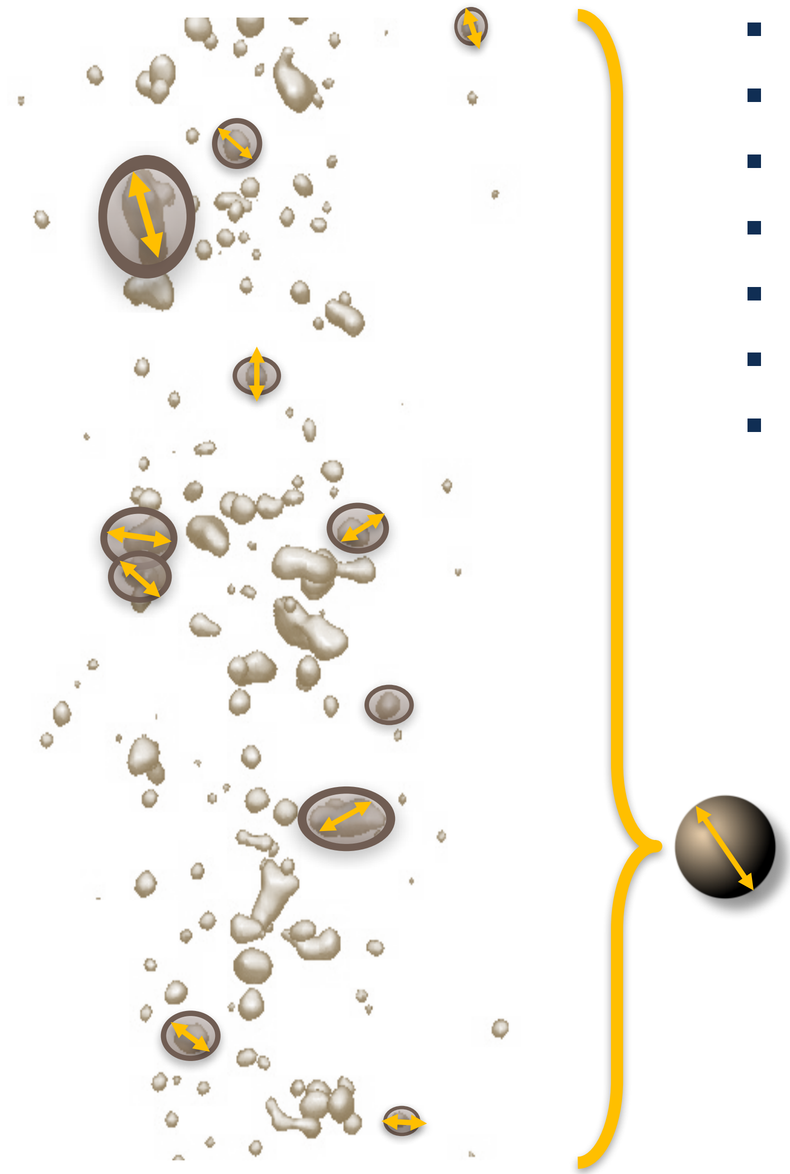

- Total Volume of Defects (V_{tot})
- Pore Volume Fraction (V_{fract})
- Spatial Location of Pores *(x, y, z)*
- Total Number of Defects *(N)*
- Total Defects/Length *(N/L)*
- Average Defect Volume ($V_{avg.}$)*
- Average Equivalent Spherical Diameter ($ESD_{avg.}$)*

How do we *best* represent the defect populations present?

Defect Quantification

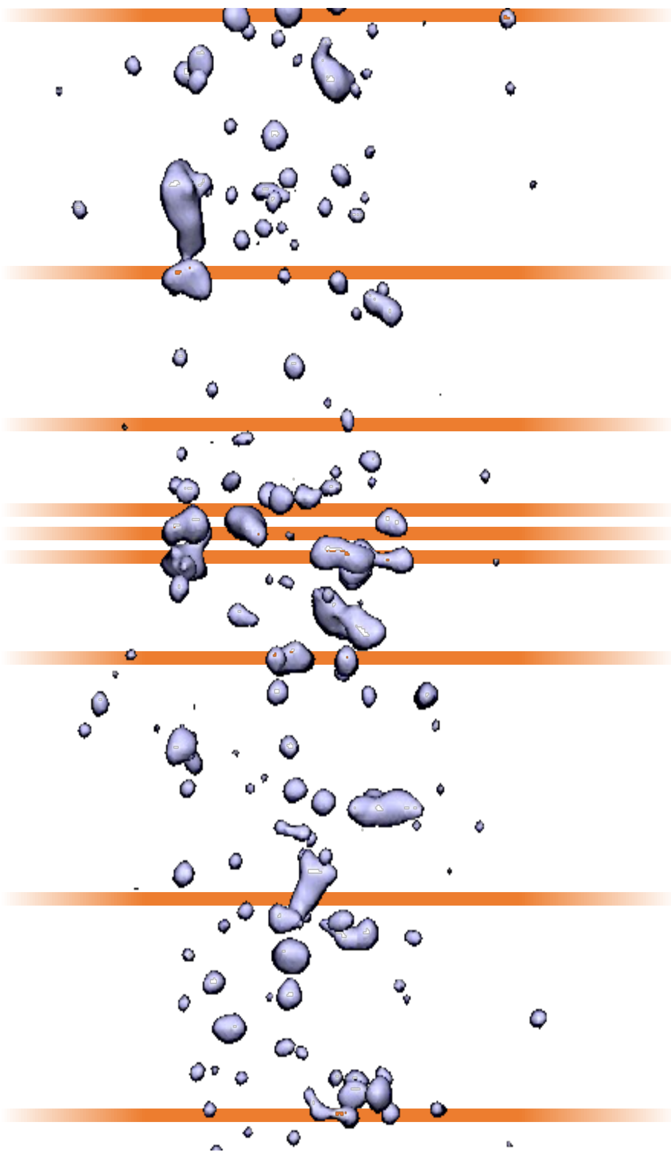

- Total Volume of Defects *(V_{tot})*
- Pore Volume Fraction *(V_{fract})*
- Spatial Location of Pores *(x, y, z)*
- Total Number of Defects *(N)*
- Total Defects/Length *(N/L)*
- Average Defect Volume (*$V_{avg.}$*)*
- Average Equivalent Spherical Diameter (*$ESD_{avg.}$*)*
- Average Cross-Sectional Area (*$CSA_{avg.}$*)*

How do we *best* represent the defect populations present?

Defect Quantification

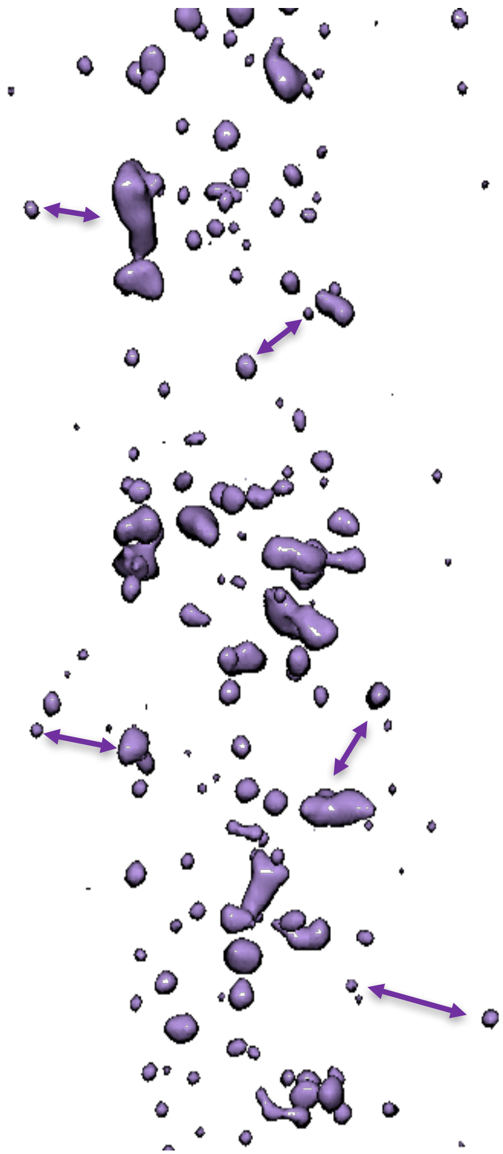

- Total Volume of Defects *(V_{tot})*
- Pore Volume Fraction *(V_{fract})*
- Spatial Location of Pores *(x, y, z)*
- Total Number of Defects *(N)*
- Total Defects/Length *(N/L)*
- Average Defect Volume ($V_{avg.}$)*
- Average Equivalent Spherical Diameter ($ESD_{avg.}$)*
- Average Cross-Sectional Area ($CSA_{avg.}$)*
- Average Nearest Neighbor Distance ($NND_{avg.}$)*

How do we *best* represent the defect populations present?

Defect Characterization

Sandia National Laboratories

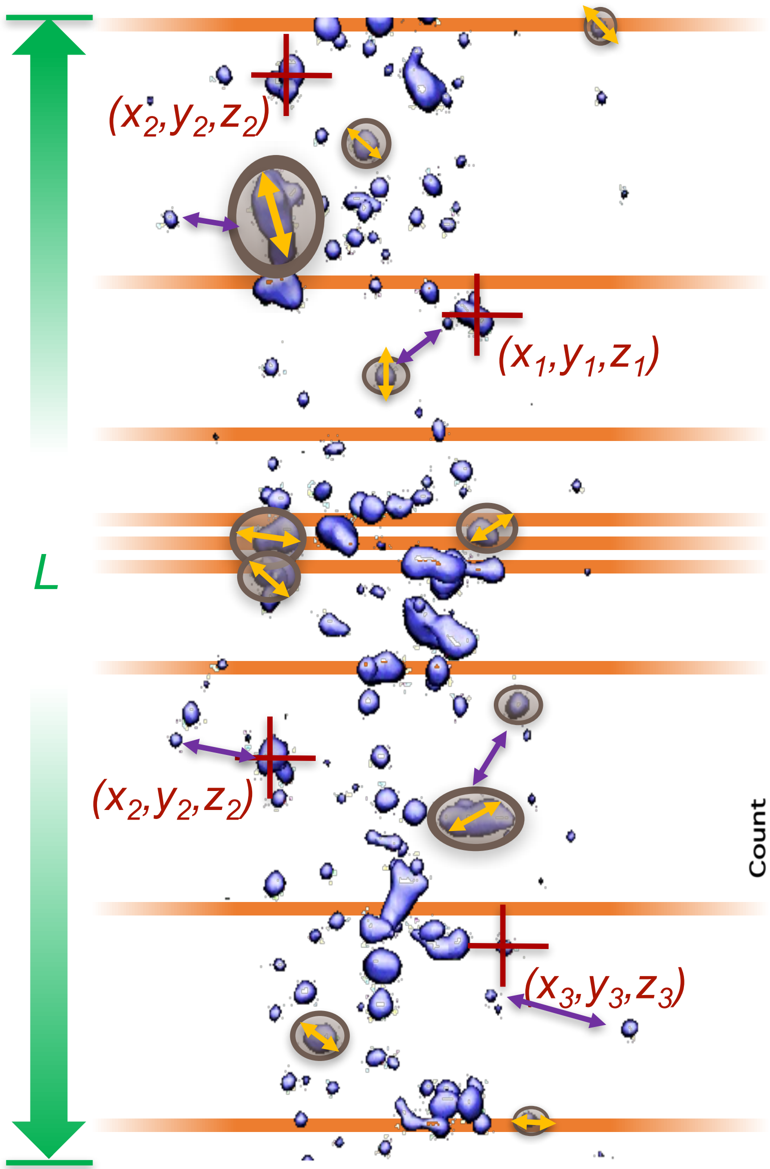

- Total Volume of Defects (V_{tot})
- Pore Volume Fraction (V_{fract})
- Spatial Location of Pores *(x, y, z)*
- Total Number of Defects *(N)*
- Total Defects/Length *(N/L)*
- Average Defect Volume ($V_{avg.}$)*
- Average Equivalent Spherical Diameter ($ESD_{avg.}$)*
- Average Cross-Sectional Area ($CSA_{avg.}$)*
- Average Nearest Neighbor Distance ($NND_{avg.}$)*

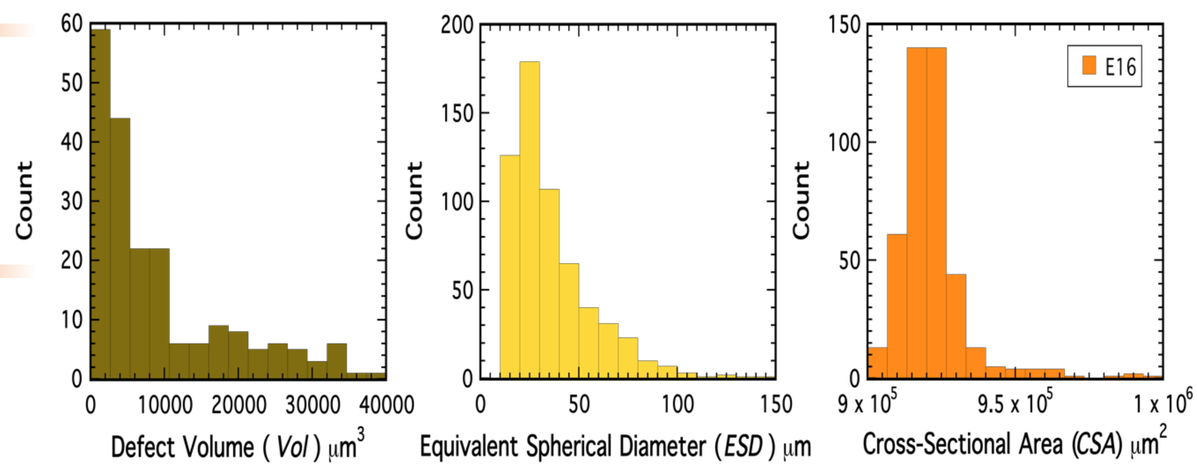

Interior Subsampling

Sandia National Laboratories

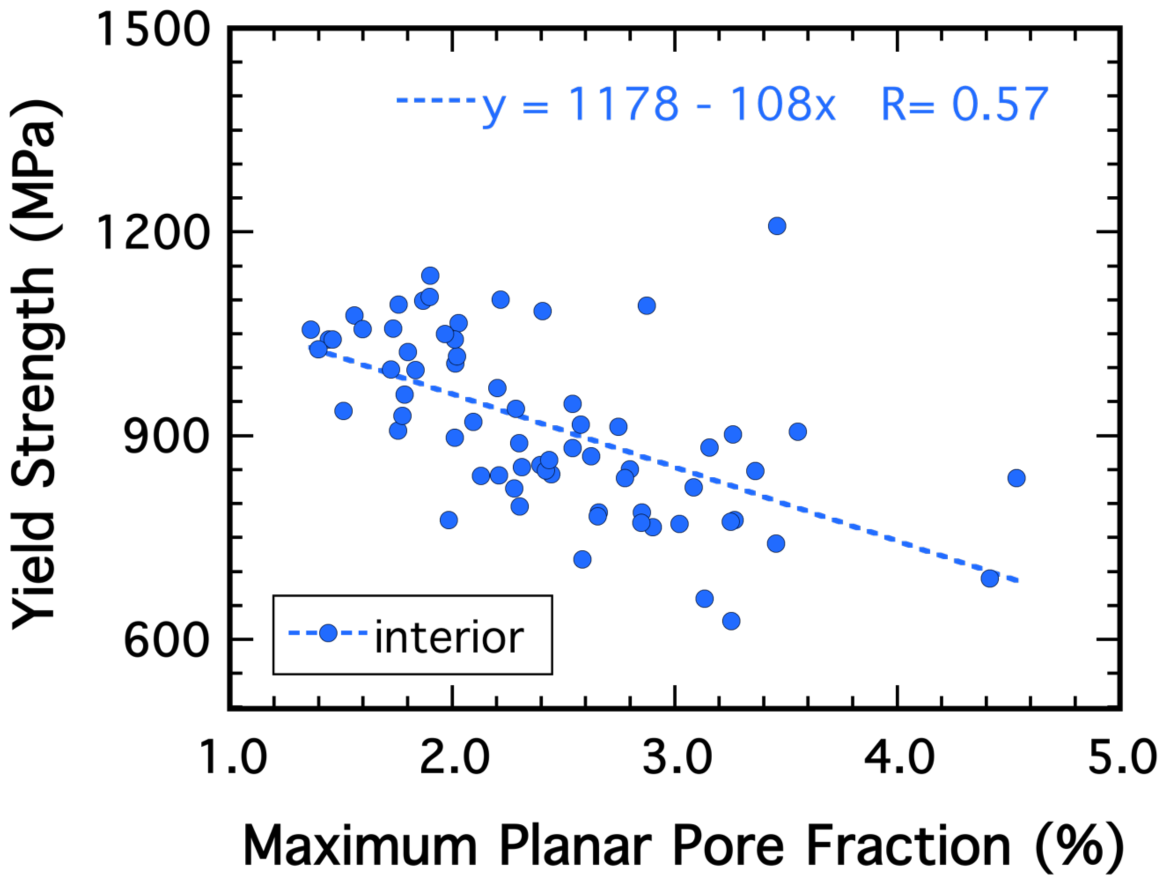

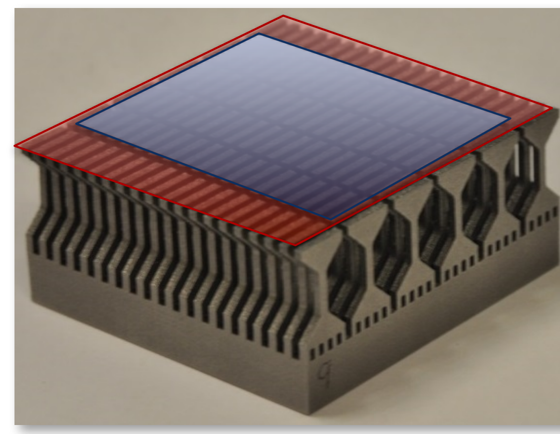

Individual Correlations with YS

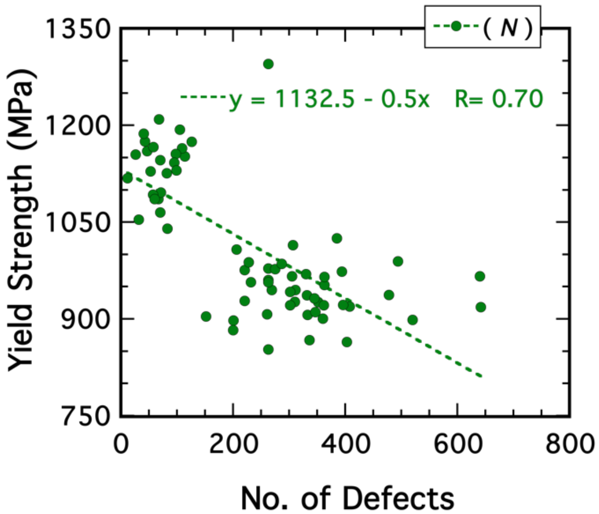

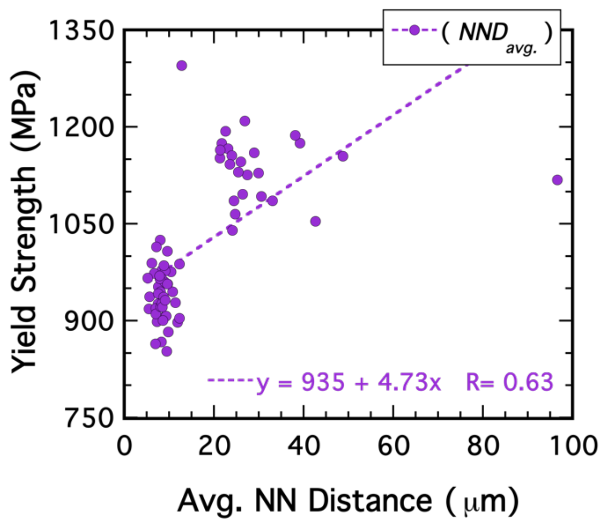

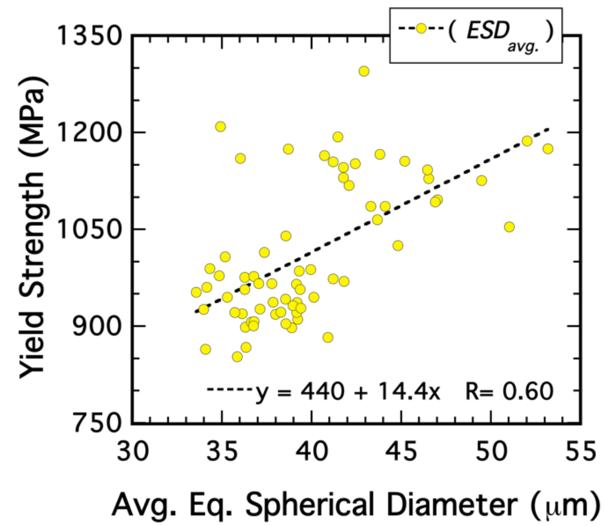

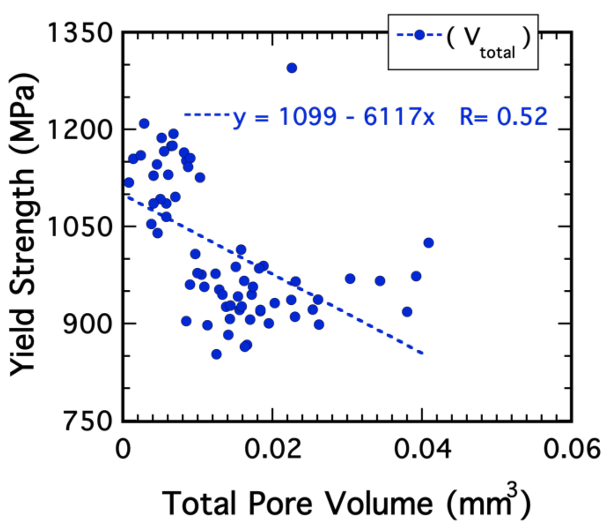

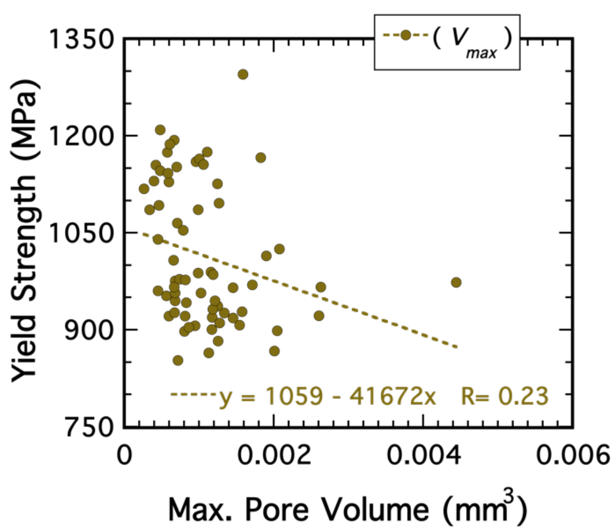

In relation to Y.S.

Measure	R value	R^2
No. of Defects	-0.705	0.50
Avg. NN Distance (mm)	0.631	0.40
Avg. ESD (mm)	0.601	0.36
Max CSA Redux (mm^2)	-0.581	0.38
Total Pore Volume (mm^3)	-0.518	0.27
Avg. Defect Vol. (mm^3)	0.500	0.25
Max CSA Redux (%)	-0.486	0.24
Maximum Pore Size	-0.257	0.07

Multivariate Regression

In relation to Y.S.

No. of Descriptors	R^2	No. of Defects (*N*)	Avg. Defect Volume ($V_{avg.}$)	Avg. Equivalent Spherical Diameter ($ESD_{avg.}$)	Total Pore Volume (V_{tot})	Maximum Pore Volume (V_{max})	Average Nearest Neighbor Distance ($NND_{avg.}$)	Maximum Cross-Sectional Area Reduction (CSA_{redux})
1	**.497**	X						
1	.398						X	
2	**.548**	X		X				
2	.542	X	X					
3	.579	X	X					X
3	.579	X		X				X
4	**.594**	X	X				X	X
4	.594	X			X		X	X
5	.604	X	X		X		X	X
5	.603	X		X	X		X	X
6	.604	X	X	X	X		X	X
6	.604	X		X	X	X	X	X
7	.604	X	X	X	X	X	X	X

$\sigma_{ys} = 1132 - 0.5(\boldsymbol{N})$ $R^2 \sim 0.5$

$\sigma_{ys} = 835 - 0.382\,(\boldsymbol{N}) + 6.74\,(\boldsymbol{ESD_{avg.}})$ $R^2 \sim 0.55$

$\sigma_{ys} = 963 - 0.431\,(\boldsymbol{N}) + 5.33\,(\boldsymbol{ESD_{avg.}}) + 3132\,(\boldsymbol{V_{tot}}) - 0.005\,(\boldsymbol{CSA_{redux}})$ $R^2 \sim 0.6$

*Boyce, et al., **Adv. Engr. Mat.** vol. 19 (2017) pp. 1-10*

Conclusions

- Variation in chemical composition and surface finish between two independently vendor-produced AM lots of PH 17-4 were observed. These differences contributed to large variations in load-displacement behavior and distinctively different failure modes between both lots.

- Within one set of AM PH 17-4 stainless steel examined, total quantity of pores was the most strongly correlated pore metric relative to yield strength. Total quantity of pores exhibited a correlation coefficient (R) of 0.7 and a maximum coefficient of determination (R^2) of 0.5

- Using multivariate regression, combinatorial predictions of yield stress, as a function of multiple porosity metrics, are possible but cumulatively only account for approximately 60% of variability observed.
  - With two measures, a coefficient of determination ($\sim R^2$) of 0.55 was achieved
  - With four measures, a coefficient of determination ($\sim R^2$) of 0.60 was achieved

Questions

1. B. Salzbrenner, J. Rodelas, J. Madison, B. Jared, L. Swiler, Y-L. Shen, B. Boyce, *"High-Throughput Stochastic Tensile Performance of Additively Manufactured Stainless Steel"* **JOURNAL OF MATERIALS PROCESSING TECHNOLOGY,** vol. 241, (2017) pp. 1-12 doi: 10.1016/j.jmatprotec.2016.10.023

2. B. Boyce, B. Salzbrenner, J. Rodelas, L. Swiler, J. Madison, B. Jared, Y-L. Shen, *"Extreme-Value Statistics Reveal Failure-Critical Defects in Additive Manufacturing"* **ADVANCED ENGINEERING MATERIALS,** vol. 19, issue 4, (2017) pp. 1-10 doi: 10.1002/adem.201700102

Gen 2

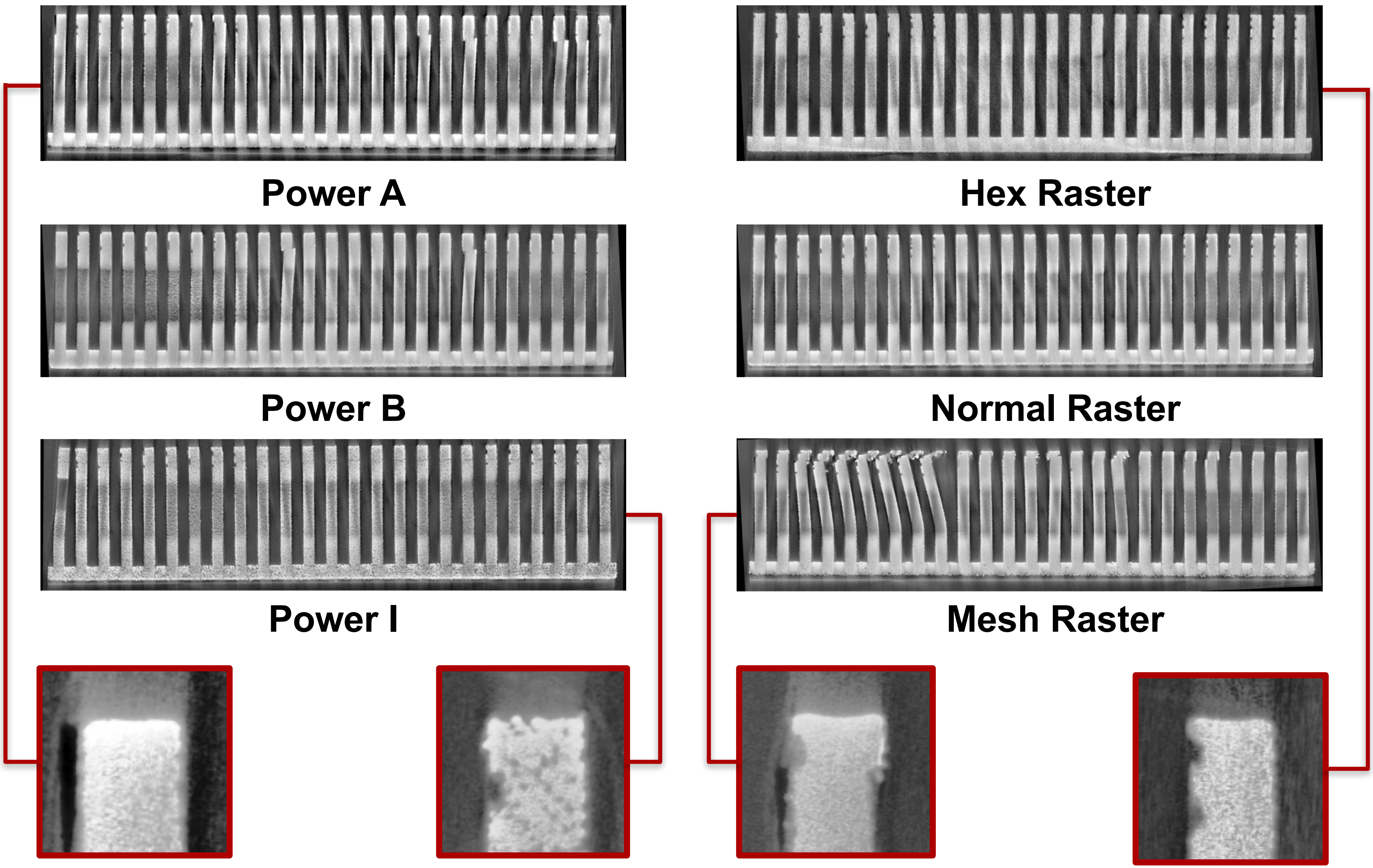

Load-Bearing Area